AIMS Mathematics, 11(1): 2088–2110.
DOI: 10.3934/math.2026086
Received: 10 November 2025
Revised: 10 January 2026
Accepted: 13 January 2026
Published: 22 January 2026

https://www.aimspress.com/journal/Math

Research article

Construction of new wave patterns for the (3+1)-dimensional Kadomtsev–Petviashvili equation using a couple of integrating architectures

Saud Owyed*

Department of Mathematics, College of Science, University of Bisha, Bisha 61922, Saudi Arabia

* **Correspondence:** Email: saalgamdi@ub.edu.sa.

Abstract: The aim of this study is to extract new exact solutions for the Kadomtsev–Petviashvili (KP) equation in three spatial dimensions and one time dimension, which is widely used in quantum field theory and plasma physics. This research refers to two separate methods–the generalized Arnous (GA) method and the $\frac{G'}{bG'+G+a}$ expansion method to uncover various new soliton solutions for the given model. These solutions are usually expressed as rational, trigonometric, and hyperbolic functions, which increase the usefulness of the method for practical applications. In addition, the conditions certifying that these solutions remain valid are also identified. The behavior of these solutions is shown through a visual representation. The recorded results are new and show how both methods are effective and robust, making them valuable tools for solving various differential equations in applied sciences and engineering.

Keywords: (3+1)-dimensional Kadomtsev–Petviashvili equation; generalized Arnous method; $\frac{G'}{bG'+G+a}$-expansion method; bright soliton; singular soliton; dark soliton
Mathematics Subject Classification: 35C08, 35R11, 37K40

1. Introduction

Nonlinear partial differential equations (PDEs) appear in many different physical situations, such as fluid dynamics, plasma physics [1], solid mechanics, and quantum field theory [2]. In addition, systems of these equations are found in the chemical and biological fields. The study of nonlinear wave equations and the concept of solitons have led to important progress in applied sciences [3]. Solitary waves and solitons appear in many different areas, such as shallow water and deep water waves, optical communications, Bose–Einstein condensates, and biological models [4]. Solitary waves are waves that maintain their shape as they move, usually originating from a specific type of nonlinear

partial differential equation. A soliton is a special kind of solitary wave that maintains its shape even after colliding with another soliton, which means that the collision is inelastic. Both solitary waves and solitons maintain their shape as they travel long distances. John Scott Russell was the first who noticed these waves, which led to the introduction of the soliton [5]. Due to its stability over a long period of time, it caught the attention of engineers, mathematicians, and physicists across the world [6]. Optical solitons [7] are one of the major areas of study in soliton theory due to their wide range of uses in communication and information technologies. Various different techniques have been introduced to find the exact solution of the nonlinear equation, such as the tanh-coth method [8], the inverse scattering transform [9], the exp-function method [10], the projective Riccati equation method [11], and the Jacobi elliptic functions method [12], the power series approach [13], the F-expansion technique [14], the Hirota bilinear method [15], the Kudryashov method [16], and many others approaches. In reality, there is no single approach that works for every type of nonlinear problem.

In our study, we focus on the (3+1)-dimensional Kadomtsev–Petviashvili (KP) equation [17]. This equation was first created by Kadomtsev and Petviashvili in 1970. It is used to describe waves in shallow water where the restoring force is not much stronger. Over time, it has become a standard model for waves that are dispersive and weakly nonlinear, mostly one-dimensional but with some slight effects in the transverse direction. The equation has ability to show how waves move in different dimensions has made it useful in various areas. The KP equation describes how waves that are not very steep and have a long wavelength change as time passes, and their movement isn't much influenced by the side-to-side direction. Now, a benchmark model for waves that are aversive and weakly nonlinear, primarily one-dimensional but with some weak transverse effects, has emerged. The equation can explain how waves behave in different dimensions, which makes it particularly useful in many distinct areas.

The general form of the KP equation in (2+1) dimensions can be written as

$$(u_t + 6\,u\,u_x + u_{xxx})_x + 3\sigma^2\,u_{yy} = 0, \tag{1.1}$$

where u is the function of x,y, and t, respectively. The classical (3+1)-dimensional KP-I and KP-II equations differ from each other based on the sign of their dispersion terms

$$\sigma = \pm 1,$$

which can be either positive or negative.

The general form of the KP-type equation in (3+1) dimensions is

$$(u_t + 6uu_x + u_{xxx})_x - 3u_{yy} - 3u_{zz} = 0, \tag{1.2}$$

where $u(x, y, z, t)$ stands for the wave shape or the amplitude of the wave, which is a function of the three space coordinates x, y, and z, respectively. Subscripts denote the partial derivatives in the equation.

Many scholars have spent years looking into the behavior and different types of solutions for the standard (3+1) KP equation and its related forms [18], highlighting how important it is for many real-world uses. In a study, researchers found rogue waves and bright-dark solitons, and they looked into how these structures behave dynamically. Ablowitz and Segur [19] showed how useful it is to look at how wave packets interact in fluid systems, where the effects that occur in different directions are very important. Agrawal [20] focused on the (3+1) KP equation when looking at how solitons

move and how their spectra spread out in optical fibers, where effects that occur across the width of the fiber can greatly affect how pulses behave. Grimshaw [21] said that the equation helps to explain how energy moves and mixes in the ocean by showing how internal waves change over time in three dimensions. Ramani et al. [22] proposed that the classical (3+1) KP equation is conditionally integrable with respect to its integrability. Later, Porsezian et al. [23] offered more evidence for its possible integrability using the Painlevé test. Ma [24] constructed the N-soliton solutions of the equation using the Hirota bilinear method. Recently, Wazwaz and Xu [25] introduced a new integrable generalized (n+1)-dimensional KP extension. Using this extension, they discovered infinite conservation laws, N-soliton solutions, Lax pairings, and Bäcklund transformations. Table 1 summarizes recently published studies on the (3+1)-dimensional KP equation, including the equation type, the solution methods employed, and the main obtained results.

Table 1. Comparison of recent works on (3+1)-dimensional KP equation.

Author's (year)	Equation type	Method	Obtained results	Ref.
Li et al. (2025)	(3+1)-dimensional modified KP	∂-formalism nonlinear Fourier transform, spectral analysis	Framework of solving IVP, integrable MKP structure (no explicit soliton family listed in the abstract)	[26]
Alhejaili et al. (2025)	Two new extended (3+1) KP equations	Painlevé test, simplified Hirota linear method	Multiple soliton and lump solutions	[27]
Ahamed and Sinuvasan (2025)	(3+1) (gKP) equation with arbitrary nonlinearity $f(u)$	Lie symmetries, optimal system, reduction	Invariant solutions, solitary wave, elliptic and Jacobi function representations	[28]
Mohammed et al. (2025)	(3+1)-dimensional Boussinesq KP-type (B-KP) equation	Improved modified extended tanh-function method	Dark, bright, singular solitons; singular periodic, Jacobi elliptic rational, exponential waves	[29]
Alhejaili et al. (2024)	(3+1)-dimensional Boussinesq KP-type, separated (3+1) Boussinesq and (3+1) KP equations	Simplified Hirota method, tanh and tan methods	Multiple soliton, lump, traveling, wave, shock, and periodic solutions	[30]

No doubt, the proposed equation was studied widely, but the exact solution of the equation has not been found using these methods. The present work aims to find various types of exact solutions for the equation given as 1.2 and to study their physical properties in depth. Finding exact solutions for the KP equation helps to understand how the system described by the equation behaves. These solutions can show important features, such as the presence of certain wave types, solitons, or other stable structures, which help explain the behavior of the system. This ability to predict is very useful in areas such as fluid dynamics, plasma physics, and nonlinear optics.

In this study, we want to address a gap in the existing research by providing the precise soliton solutions for the new extended (3+1)-dimensional KP equation using the generalized Arnous (GA) method [31] and the $\frac{G'}{bG'+G+a}$ expansion method [32]. We first introduce general solutions using

GA method and the $\frac{G'}{bG'+G+a}$ expansion method along with a proper traveling wave transformation. Different types of soliton solutions are obtained, which helps in understanding the behavior of the KP equation with these methods. These methods have been widely used before to solve nonlinear equations, and many studies have shown how well they work. Our findings offer new insights into how these solutions develop over time. The GA method and the $\frac{G'}{bG'+G+a}$ expansion method offer several advantages over conventional analytical techniques used for nonlinear evolution equations. By eliminating time-consuming bilinear transformations or intricate symbolic computations, these techniques offer a more straightforward and methodical derivation process. Moreover, they are capable of generating a richer variety of exact solutions, including rational, trigonometric, hyperbolic, and hybrid soliton structures within a unified framework. This adaptability strengthens the analytical treatment of the model by allowing the investigation of wider parameter regimes and revealing wave characteristics that are difficult to reach using conventional techniques.

Unlike many earlier studies on the KP equation, where the reported exact solutions are predominantly limited to single-soliton, periodic, or simple traveling wave forms expressed through standard hyperbolic or trigonometric functions under relatively restrictive parameter constraints, the present work introduces several fundamentally new features. Specifically, by using the $\frac{G'}{bG'+G+a}$ expansion method and the GA method, we obtain novel functional forms that are not found in earlier studies, such as parameter-dependent hybrid solutions, mixed trigonometric hyperbolic structures, and higher order rational solutions. Furthermore, the constraint conditions ensuring the validity of these solutions are significantly relaxed, leading to a broader admissible parameter space and allowing the emergence of additional soliton types, such as singular solitons, interacting multi-soliton configurations, and localized wave patterns. There are many known solutions like Hirota solitons, lump solutions, rogue waves, and multi-soliton structures in the literature. To show the novelty of our results, we compare our solution with these well-known ones. When we remove the trigonometric parameters and keep the transverse variables fixed, our solutions become similar to single-soliton or multi-soliton forms that come from the Hirota bilinear method.

This describes that our approach is correct and that it can also be used to find the classical soliton solutions. Moreover, lump and rogue wave solutions of the KP equation are localized in all directions, meaning that they are spread out but not oscillating. However, the solutions we found in this work have a mix of exponential and periodic components, creating wave patterns that are both localized and oscillating. These patterns are different from standard lump or rogue wave solutions. These differences make it evident that the solutions obtained in this work expand and broaden previous findings in the literature, improving the analytical comprehension of the KP equation and its applications in quantum field theory and plasma physics.

The organization of the paper is as follows: Section 2 discusses a general idea of the methodology of both methods. Section 3 explains the mathematical evaluation of methods and their different types of solutions. In Section 4, we study the formation of graphs and figures. In section 5, modulation instability is discussed. Section 6 encapsulates the primary findings and proposes possible extensions of this research to other multidimensional nonlinear models.

2. Methodology

The GA method is an analytical technique that is useful for securing exact solutions of a wide range of nonlinear PDEs. The $\frac{G'}{bG'+G+a}$ expansion method is a straightforward and effective mathematical approach used to generate traveling wave solutions for nonlinear evolution equations.

Suppose that the general nonlinear PDE is as follows:

$$\Phi(u,\ u_x,\ u_t,\ u_y,\ u_z,\ u_{xx},\ u_{tt},\ u_{yy},\ u_{zz},\ u_{xt},\ u_{xy},\ u_{xz},\ u_{yz},\ u_{yt},\ \dots) = 0, \tag{2.1}$$

where Φ denotes a polynomial (multivariate) in the field $u(x, y, z, t)$ and its partial derivatives. We must reduce the given PDE to an ordinary differential equation (ODE) using a suitable wave transformation.

$$u = U(\eta) = U(kx + ly + mz - \omega t), \quad \eta = kx + ly + mz - \omega t, \tag{2.2}$$

where k, l, and m are the wave numbers in the x, y, and z directions. Here ω, is the wave frequency, and all are constants. We obtain the ODE in the form of

$$P(U, U', U'', U''', \dots) = 0, \tag{2.3}$$

where ($'$) denotes the derivative with respect to η.

2.1. The GA method

This section provides a summary of the fundamental steps in the GA method.

Step 1. Let us suppose that the solution for Eq (2.3) is

$$U(\eta) = \alpha_0 + \sum_{i=1}^{N} \frac{\alpha_i + \beta_i G'(\eta)^i}{G(\eta)^i}, \tag{2.4}$$

where α_0, α_i, and β_i act as constants, and $G(\eta)$ satisfies the condition

$$[G'(\eta)]^2 = [G(\eta)^2 - \rho]\ln(B)^2 \tag{2.5}$$

with

$$G^{(m)}(\eta) = \begin{cases} G(\eta)\ln(B)^m, & \text{if } m \text{ is even,} \\ G'(\eta)\ln(B)^{m-1}, & \text{if } m \text{ is odd,} \end{cases}$$

where $m \geq 2$ and $0 < B < 1$.

The following ODE has the solution in the form of

$$G(\eta) = \kappa \ln(B) B^{\eta} + \frac{\rho}{4\kappa \ln(B) B^{\eta}}, \tag{2.6}$$

where κ and ρ are any parameters.

Step 2. N can be found by using the rule that balances the equation involving the highest order derivative and the highest degree of the non-linear term.

Step 3. Following the substitution of Eqs (2.4) and (2.5) into Eq (2.3), and given that

$$G(\eta) \neq 0,$$

this substitution produces a polynomial in $\frac{1}{G'(\eta)}$, $\frac{G'(\eta)}{G(\eta)}$, and $G(\eta)$.

Next, all terms with identical powers are collected and set equal to zero. Subsequently, ρ, κ, ω, α_0, α_1, α_2, β_1, and β_2 are found by solving the system. Using Eqs (2.5) and (2.2), the solutions can be obtained for Eq (2.1).

2.2. $\frac{G'}{bG'+G+a}$ *expansion method*

Step 1. Let us suppose that the solution of the transformed ODE is

$$U(\eta) = \sum_{i=0}^{N} AiF^i, \tag{2.7}$$

where

$$F = F(\eta) = \frac{G'}{bG'+G+a}$$

and $a, b \neq 0$. A_i are arbitrary constants that will be found later.

F satisfies the requirement.

$$F' = \frac{dF(\eta)}{d\eta} = (\lambda - \mu - 1)F^2 + \frac{2\mu - \lambda}{b} - \frac{\mu}{b^2}, \tag{2.8}$$

and the ODE has the solution in this form:

$$G'' = -\frac{\lambda}{b}G' - \frac{\lambda}{b^2}G - \frac{\mu}{b^2}a, \tag{2.9}$$

where λ and μ are considered real numbers.

Step 2. The positive integer N can be determined by applying the principle of balancing the highest order derivative with the non-linear term in Eq (2.3).

Step 3. Two types of solutions are considered for Eq (2.9).

Type 1. If

$$\vartheta = \lambda^2 - 4\mu > 0,$$

then

$$G = -a + m_1 e^{\frac{1}{2b}(-\lambda - \sqrt{\vartheta})\eta} + m_2 e^{\frac{1}{2b}(-\lambda + \sqrt{\vartheta})\eta},$$

m_1, and m_2 are arbitrary constants that satisfy

$$a^2 + m_1^2 + m_2^2 \neq 0.$$

In this type, $F = F(\eta)$ can be written as

$$F = \frac{m_1(\lambda + \sqrt{\vartheta}) + m_2(\lambda - \sqrt{\vartheta})e^{\frac{\sqrt{\vartheta}}{b}\eta}}{b\, m_1(\lambda - 2 + \sqrt{\vartheta}) + b\, m_2(\lambda - 2 - \sqrt{\vartheta})e^{\frac{\sqrt{\vartheta}}{b}\eta}}. \tag{2.10}$$

We can also write $F = F(\eta)$ as

$$F = \frac{R_1 \sinh(\frac{\sqrt{\vartheta}}{2b}\eta) + R_2 \cosh(\frac{\sqrt{\vartheta}}{2b}\eta)}{R_3 \sinh(\frac{\sqrt{\vartheta}}{2b}\eta) + R_4 \cosh(\frac{\sqrt{\vartheta}}{2b}\eta)}. \tag{2.11}$$

Here,

$$\begin{aligned}
\lambda(m_2 - m_1) - \sqrt{\vartheta}(m_2 + m_1) &= R_1,\\
\lambda(m_2 + m_1) - \sqrt{\vartheta}(m_2 - m_1) &= R_2,\\
b(\lambda - 2)(m_2 - m_1) - \sqrt{\vartheta}(m_2 + m_1) &= R_3,\\
b(\lambda - 2)(m_2 + m_1) - \sqrt{\vartheta}(m_2 - m_1) &= R_4.
\end{aligned}$$

- If

$$(\lambda - 2)(m_2 - m_1) - \sqrt{\vartheta}(m_2 + m_1) = 0,$$

then

$$F = \frac{\lambda - 2\mu}{2bQ} - \frac{\sqrt{\vartheta}}{2bQ}\tanh(\frac{\sqrt{\vartheta}}{2b}\eta). \tag{2.12}$$

Here,

$$Q = \lambda - \mu - 1.$$

- If

$$(\lambda - 2)(m_2 + m_1) - \sqrt{\vartheta}(m_2 - m_1) = 0,$$

then

$$F = \frac{\lambda - 2\mu}{2bQ} - \frac{\sqrt{\vartheta}}{2bQ}\coth(\frac{\sqrt{\vartheta}}{2b}\eta). \tag{2.13}$$

Type 2. If

$$\vartheta = \lambda^2 - 4\mu < 0,$$

then

$$G = -a + e^{\frac{-\lambda}{2b}\eta}\left(m_1 \cos(\frac{\sqrt{-\vartheta}}{2b}\eta) + m_2 \sin(\frac{\sqrt{-\vartheta}}{2b}\eta)\right).$$

In this type, $F = F(\eta)$ has the following representation

$$F = \frac{S_1 \cos(\frac{\sqrt{-\vartheta}}{2b}\eta) + S_2 \sin(\frac{\sqrt{-\vartheta}}{2b}\eta)}{S_3 \cos(\frac{\sqrt{-\vartheta}}{2b}\eta) + S_4 \sin(\frac{\sqrt{-\vartheta}}{2b}\eta)}. \tag{2.14}$$

Here,

$$\begin{aligned}
\lambda m_1 - \sqrt{-\vartheta} m_2 &= S_1,\\
\lambda m_2 - \sqrt{-\vartheta} m_1 &= S_2,\\
b\left((\lambda - 2)m_1 - \sqrt{-\vartheta} m_2\right) &= S_3,\\
b\left((\lambda - 2)m_2 + \sqrt{-\vartheta} m_1\right) &= S_4.
\end{aligned}$$

- If

$$(\lambda - 2)m_2 + \sqrt{-\vartheta}m_1 = 0,$$

then

$$F = \frac{\lambda - 2\mu}{2bQ} + \frac{\sqrt{-\vartheta}}{2bQ}\tan(\frac{\sqrt{-\vartheta}}{2b}\eta). \tag{2.15}$$

- If

$$(\lambda - 2)m_1 - \sqrt{-\vartheta}m_2 = 0,$$

then

$$F = \frac{\lambda - 2\mu}{2bQ} - \frac{\sqrt{-\vartheta}}{2bQ}\cot(\frac{\sqrt{-\vartheta}}{2b}\eta). \tag{2.16}$$

Step 4. Substitute Eqs (2.8) and (2.9) into the transformed ODE and set the coefficients of F^i to zero. This gives a system of equations. The values of the unknown constants can be found by solving this set of equations.

3. Mathematical evaluation

In this section, we will extract the exact solution of the KP equation using the proposed methods. Consider the wave transformation

$$u = U(\eta), \quad \eta = kx + ly + mz - \omega t. \tag{3.1}$$

Extract u', u'', u''' and u'''' from Eq (3.1) and substitute it into Eq (1.2); we obtain

$$k^4U^{(4)}(\eta) + U''(\eta)\left(6k^2U(\eta) - k\omega - 3\left(l^2 + m^2\right)\right) + 6k^2U'(\eta)^2 = 0. \tag{3.2}$$

Integrating the above equation twice with respect to η, and without loss of generality, the constant is set to zero. This corresponds to a translational invariance of the wave pattern that does not affect the overall shape or main features of the solution. We obtain the ODE in this form:

$$k^4U''(\eta) + 3k^2U(\eta)^2 - k\omega U(\eta) - 3l^2U(\eta) - 3m^2U(\eta). \tag{3.3}$$

Using the balancing principle, the terms U^2 and U'' in Eq (3.3) result in

$$N = 2.$$

3.1. Solutions by GA method

As

$$N = 2,$$

the solution is

$$U(\eta) = \alpha_0 + \frac{\alpha_1 + \beta_1 G'(\eta)}{G(\eta)} + \frac{\alpha_2 + \beta_2 (G'(\eta))^2}{G(\eta)^2}, \tag{3.4}$$

where $\alpha_0, \alpha_1, \alpha_2, \beta_1$, and β_2 are constants and β_2 does not equal to zero. By substituting Eq (3.4) into

Eq (3.3) and equating the coefficients of $\frac{1}{G'(\eta)}$ and $\frac{G'(\eta)}{G(\eta)}$, a system of algebraic equations is formed.

$$
\begin{aligned}
&6\alpha_1\beta_1k^2 = 0,\\
&6\alpha_1\alpha_2k^2 - 2\alpha_1k^4\rho\ln^2(B) - 6\alpha_1\beta_2k^2\rho\ln^2(B) = 0,\\
&6\alpha_2\beta_1k^2 - 2\beta_1k^4\rho\ln^2(B) - 6\beta_1\beta_2k^2\rho\ln^2(B) = 0,\\
&6\alpha_0\beta_1k^2 + 6\beta_1\beta_2k^2\ln^2(B) - \beta_1k\omega - 3\beta_1l^2 - 3\beta_1m^2 = 0,\\
&\alpha_1k^4\ln^2(B) + 6\alpha_0\alpha_1k^2 + 6\alpha_1\beta2k^2\ln^2(B) - \alpha_1k\omega - 3\alpha_1l^2 - 3\alpha_1m^2 = 0,\\
&6\beta_2k^4\rho^2\ln^4(B) - 6\alpha_2k^4\rho\ln^2(B) + 3\alpha_2^2k^2 - 6\alpha_2\beta_2k^2\rho\ln^2(B) + 3\beta_2^2k^2\rho^2\ln^4(B) = 0,\\
&3\alpha_0^2k^2 - 3\alpha_0m^2 + 6\alpha_0\beta_2k^2\ln^2(B) + 3\beta_1^2k^2\ln^2(B) + 3\beta_2^2k^2\ln^4(B) - \alpha_0k\omega\\
&- \beta_2k\omega\ln^2(B) - 3\alpha_0l^2 - 3\beta_2l^2\ln^2(B) - 3\beta_2m^2\ln^2(B) = 0,\\
&4\alpha_2k^4\ln^2(B) - 4\beta_2k^4\rho\ln^4(B) + 6\alpha_0\alpha_2k^2 - 6\alpha_0\beta_2k^2\rho\ln^2(B) + 3\alpha_1^2k^2 + 6\alpha_2\beta_2k^2\ln^2(B)\\
&- 3\beta_1^2k^2\rho\ln^2(B) - 6\beta_2^2k^2\rho\ln^4(B) - \alpha_2k\omega + \beta_2k\rho\omega\ln^2(B) - 3\alpha_2l^2 + 3\beta_2l^2\rho\ln^2(B)\\
&- 3\alpha_2m^2 + 3\beta_2m^2\rho\ln^2(B) = 0.
\end{aligned}
$$

With the help of a mathematical tool, we obtain the solutions

$$
\textbf{Set 1}\ \begin{Bmatrix} \alpha_0 = -\beta_2ln^2(B),\ \alpha_1 \to 0,\ \alpha_2 = \rho ln^2(B)(\beta_2 + 2k^2), \\ \beta_1 = 0,\ \omega = \dfrac{4k^4ln^2(B) - 3l^2 - 3m^2}{k}, \end{Bmatrix}
$$

and

$$
\textbf{Set 2}\ \begin{Bmatrix} \alpha_0 = \frac{1}{3}\left[-3\beta_2ln^2(B) - 4k^2ln^2(B)\right],\ \alpha_1 = 0,\ \alpha_2 = \rho ln^2(B)(\beta_2 + 2k^2), \\ \beta_1 = 0,\ \omega = \dfrac{-4k^4ln^2(B) - 3l^2 - 3m^2}{k}. \end{Bmatrix}
$$

Using the set 1 in Eq (3.4), the solution is

$$
U_1(\eta) = \frac{32\kappa^2k^2\rho\ln^2(B)B^{2\eta}}{\left(\rho + 4\kappa^2\ln^2(B)B^{2\eta}\right)^2}. \tag{3.5}
$$

For Eq (1.2), we can write Eq (3.5) as

$$
u_1 = \frac{32\kappa^2k^2\rho\ln^2(B)B^{2\eta}}{\left(\rho + 4\kappa^2\ln^2(B)B^{2\eta}\right)^2}, \tag{3.6}
$$

where

$$
\eta = kx + ly + mz - \frac{4k^4ln^2(B) - 3l^2 - 3m^2}{k}t,
$$

and the graphical representation is as follows (see Figures 1 and 2):

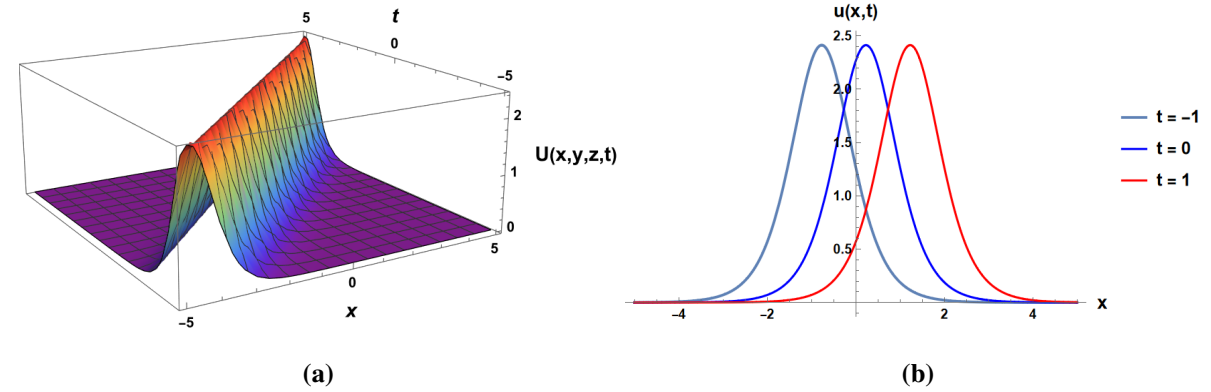

(a) **(b)**

Figure 1. $3D$ and $2D$ representations of u_1 with $\rho = 0.05$.

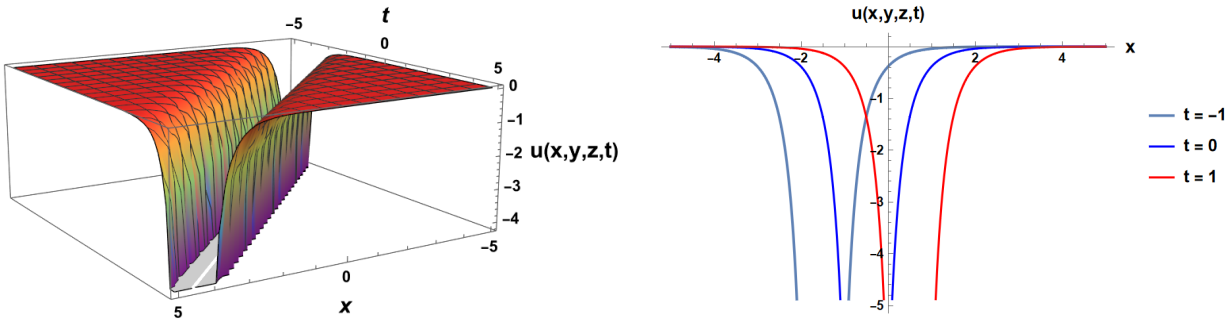

(a) **(b)**

Figure 2. $3D$ and $2D$ representations of u_1 with $\rho = -0.01$.

Using set 2 in Eq (3.4), the solution we obtained is

$$U_2(\eta) = -\frac{4k^2 \ln^2(B)\left(\rho^2 + 16\kappa^4 \ln^4(B)B^{4\eta} - 16\kappa^2\rho \ln^2(B)B^{2\eta}\right)}{3\left(\rho + 4\kappa^2 \ln^2(B)B^{2\eta}\right)^2}. \tag{3.7}$$

We can rewrite Eq (3.7) for Eq (1.2) as follows:

$$u_2 = -\frac{4k^2 \ln^2(B)\left(\rho^2 + 16\kappa^4 \ln^4(B)B^{4\eta} - 16\kappa^2\rho \ln^2(B)B^{2\eta}\right)}{3\left(\rho + 4\kappa^2 \ln^2(B)B^{2\eta}\right)^2}, \tag{3.8}$$

where

$$\eta = kx + ly + mz - \frac{-4k^4 ln^2(B) - 3l^2 - 3m^2}{k}t,$$

and the graphical representation is as follows (see Figures 3 and 4):

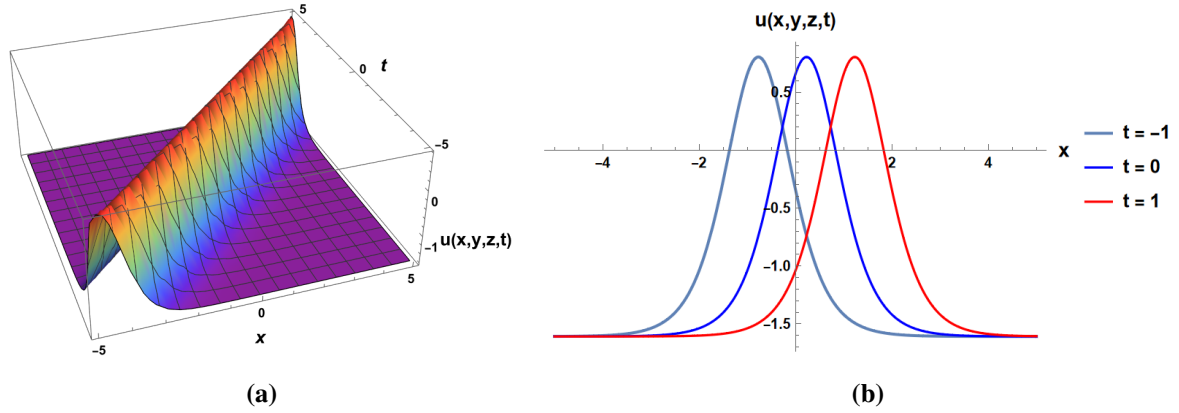

(a) **(b)**

Figure 3. $3D$ and $2D$ representations of u_2 with $\rho = 0.05$.

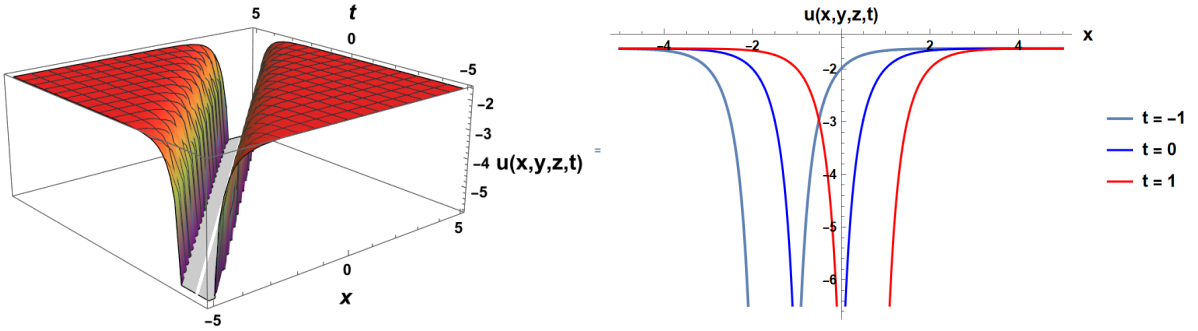

(a) **(b)**

Figure 4. $3D$ and $2D$ representations of u_2 with $\rho = -0.01$.

To check the correctness of obtained solutions, we substitute one solution in a given equation. We calculate all the necessary derivatives step by step, and after simplifying, the left-hand side of the equation becomes zero. This shows that the solution we found is exactly correct for the equation.

3.2. *Solutions by* $\dfrac{G'}{bG' + G + a}$ *expansion method*

As $N = 2$, the solution is

$$U(\eta) = A_0 + A_1 F + A_2 F^2, \tag{3.9}$$

where A_0, A_1, and A_2 are constants that can be found later and $A_2 \neq 0$. So, put Eqs (2.8) and (3.9) into Eq (3.3) and equate the coefficients of the power of F, and a system of equations is formed.

$$3A_0^2k^2 - A_0k\omega - 3A_0l^2 - 3A_0m^2 + \frac{A_1\lambda k^4\mu}{b^3} - \frac{2A_1k^4\mu^2}{b^3} + \frac{2A_2k^4\mu^2}{b^4} = 0,$$
$$3A_2^2k^2 + 6A_2\lambda^2k^4 - 12A_2\lambda k^4\mu - 12A_2\lambda k^4 + 6A_2k^4\mu^2 + 12A_2k^4\mu + 6A_2k^4 = 0,$$
$$6A_0A_1k^2 - A_1k\omega - 3A_1l^2 - 3A_1m^2 + \frac{6A_2\lambda k^4\mu}{b^3} + \frac{A_1\lambda^2k^4}{b^2} - \frac{12A_2k^4\mu^2}{b^3}$$
$$- \frac{6A_1\lambda k^4\mu}{b^2} + \frac{6A_1k^4\mu^2}{b^2} + \frac{2A_1k^4\mu}{b^2} = 0,$$

$$6A_1A_2k^2 + 2A_1\lambda^2k^4 - 4A_1\lambda k^4\mu - 4A_1\lambda k^4 + 2A_1k^4\mu^2 + 4A_1k^4\mu + 2A_1k^4 - \frac{10A_2\lambda^2k^4}{b}$$
$$+ \frac{30A_2\lambda k^4\mu}{b} + \frac{10A_2\lambda k^4}{b} - \frac{20A_2k^4\mu^2}{b} - \frac{20A_2k^4\mu}{b} = 0,$$
$$6A_0A_2k^2 + 3A_1^2k^2 - A_2k\omega - 3A_2l^2 - 3A_2m^2 - \frac{3A_1\lambda^2k^4}{b} + \frac{9A_1\lambda k^4\mu}{b} + \frac{3A_1\lambda k^4}{b} - \frac{6A_1k^4\mu^2}{b}$$
$$- \frac{6A_1k^4\mu}{b} + \frac{4A_2\lambda^2k^4}{b^2} - \frac{24A_2\lambda k^4\mu}{b^2} + \frac{24A_2k^4\mu^2}{b^2} + \frac{8A_2k^4\mu}{b^2} = 0.$$

Solving this system with Mathematica, we get

$$\textbf{Set 1}\ \begin{Bmatrix} A_0 = -\dfrac{2k^2\mu(-\lambda+\mu+1)}{b^2}, & A_1 = \dfrac{2k^2(\lambda^2-3\lambda\mu-\lambda+2\mu^2+2\mu)}{b}, \\ A_2 = -2k^2(\lambda-\mu-1)^2, & \omega = \dfrac{-3b^2l^2-3b^2m^2+\lambda^2k^4-4k^4\mu}{b^2k}, \end{Bmatrix}$$
$$\textbf{Set 2}\ \begin{Bmatrix} A_0 = -\dfrac{k^2(\lambda^2-6\lambda\mu+6\mu^2+2\mu)}{3b^2}, & A_1 = \dfrac{2k^2(\lambda^2-3\lambda\mu-\lambda+2\mu^2+2\mu)}{b}, \\ A_2 = -2k^2(\lambda-\mu-1)^2, & \omega = \dfrac{-3b^2l^2-3b^2m^2-\lambda^2k^4+4k^4\mu}{b^2k}. \end{Bmatrix}$$

Set 1.
Case 1. If

$$\vartheta = \lambda^2 - 4\mu > 0,$$

then

$$u_1 = -\frac{2k^2Q(bF - \mu(bFQ - \lambda + 2\mu))}{b^2}. \tag{3.10}$$

Here,

$$Q = \lambda - \mu - 1,$$

where

$$F = \frac{m_2\left(\sqrt{\vartheta} - \lambda\right)e^{\frac{\sqrt{\vartheta}\eta}{b}} - m_1\left(\lambda + \sqrt{\vartheta}\right)}{bm_2\left(-\lambda + \sqrt{\vartheta} + 2\right)e^{\frac{\sqrt{\vartheta}\eta}{b}} - bm_1\left(\lambda + \sqrt{\vartheta} - 2\right)}. \tag{3.11}$$

Then Eq (3.10) becomes

$$u_1 = \frac{2k^2Q\left(-2m_1m_2e^{\frac{\sqrt{\vartheta}\eta}{b}}\left(\lambda^2 + \vartheta - 4\mu\right) + m_2^2e^{\frac{2\sqrt{\vartheta}\eta}{b}}T + m_1^2T\right)}{\left(bm_2\left(-\lambda + \sqrt{\vartheta} + 2\right)e^{\frac{\sqrt{\vartheta}\eta}{b}} - bm_1\left(\lambda + \sqrt{\vartheta} - 2\right)\right)^2}. \tag{3.12}$$

Here,

$$T = -\lambda^2 + \vartheta + 4\mu.$$

- If

$$(\lambda - 2)(m_2 - m_1) - \sqrt{\vartheta}(m_2 + m_1) = 0,$$

then Eq (3.10) becomes

$$u_{1,1} = \frac{k^2\left(-\vartheta\tanh^2\left(\frac{\eta\sqrt{\vartheta}}{2b}\right) + \lambda^2 - 4\mu\right)}{2b^2}. \tag{3.13}$$

- If

$$(\lambda-2)(m_2+m_1)-\sqrt{\vartheta}(m_2-m_1)=0,$$

then Eq (3.10) becomes

$$u_{1,2}=\frac{k^2\left(-\vartheta\coth^2\left(\frac{\eta\sqrt{\vartheta}}{2b}\right)+\lambda^2-4\mu\right)}{2b^2}. \tag{3.14}$$

Case 2. If

$$\vartheta=\lambda^2-4\mu<0,$$

then

$$u_2=-\frac{2k^2Q(bF-\mu(bFQ-\lambda+2\mu))}{b^2}, \tag{3.15}$$

where

$$F=\frac{S_1\cos(\frac{\sqrt{-\vartheta}}{2b}\eta)+S_2\sin(\frac{\sqrt{-\vartheta}}{2b}\eta)}{S_3\cos(\frac{\sqrt{-\vartheta}}{2b}\eta)+S_4\sin(\frac{\sqrt{-\vartheta}}{2b}\eta)}. \tag{3.16}$$

Here,

$$\begin{aligned}
&\lambda m_1-\sqrt{-\vartheta}m_2=S_1,\\
&\lambda m_2-\sqrt{-\vartheta}m_1=S_2,\\
&b\left((\lambda-2)m_1-\sqrt{-\vartheta}m_2\right)=S_3,\\
&b\left((\lambda-2)m_2+\sqrt{-\vartheta}m_1\right)=S_4,
\end{aligned}$$

and it turns Eq (3.15) into this form:

$$u_2=-\frac{2k^2Q\left(\frac{b\left(S_1\cos\left(\frac{\eta\sqrt{-\vartheta}}{2b}\right)+S_2\sin\left(\frac{\eta\sqrt{-\vartheta}}{2b}\right)\right)\left(\frac{bQ\left(S_1\cos\left(\frac{\eta\sqrt{-\vartheta}}{2b}\right)+S_2\sin\left(\frac{\eta\sqrt{-\vartheta}}{2b}\right)\right)}{S_3\cos\left(\frac{\eta\sqrt{-\vartheta}}{2b}\right)+S_4\sin\left(\frac{\eta\sqrt{-\vartheta}}{2b}\right)}-\lambda+2\mu\right)}{S_3\cos\left(\frac{\eta\sqrt{-\vartheta}}{2b}\right)+S_4\sin\left(\frac{\eta\sqrt{-\vartheta}}{2b}\right)}-\mu\right)}{b^2}. \tag{3.17}$$

- If

$$(\lambda-2)m_2+\sqrt{-\vartheta}\,m_1=0,$$

then (3.17) becomes

$$u_{2,1}=\frac{k^2\left(-\vartheta\tanh^2\left(\frac{\eta\sqrt{\vartheta}}{2b}\right)+\lambda^2-4\mu\right)}{2b^2}. \tag{3.18}$$

- If

$$(\lambda-2)m_1-\sqrt{-\vartheta}\,m_2=0,$$

then (3.17) becomes

$$u_{2,2}=\frac{k^2\left(-\vartheta\coth^2\left(\frac{\eta\sqrt{\vartheta}}{2b}\right)+\lambda^2-4\mu\right)}{2b^2}. \tag{3.19}$$

Set 2.

Case 1. If

$$\vartheta = \lambda^2 - 4\mu > 0,$$

then

$$U_1 = \frac{k^2\left(-6b^2F^2(-\lambda+\mu+1)^2 + 6bFQ(\lambda-2\mu) - \lambda^2 + 6\lambda\mu - 2\mu(3\mu+1)\right)}{3b^2}, \tag{3.20}$$

where

$$F = \frac{m_2\left(\sqrt{\vartheta}-\lambda\right)e^{\frac{\sqrt{\vartheta}x}{b}} - m_1\left(\lambda+\sqrt{\vartheta}\right)}{bm_2\left(-\lambda+\sqrt{\vartheta}+2\right)e^{\frac{\sqrt{\vartheta}x}{b}} - bm_1\left(\lambda+\sqrt{\vartheta}-2\right)}. \tag{3.21}$$

Then Eq (3.20) will be transformed into

$$\begin{aligned} u_1 = \frac{k^2}{3b^2}\Bigg[&- \frac{6(\lambda-2\mu)Q\left(m_2(\lambda-\sqrt{\vartheta})e^{\frac{\sqrt{\vartheta}x}{b}} + m_1(\lambda+\sqrt{\vartheta})\right)}{m_2(-\lambda+\sqrt{\vartheta}+2)e^{\frac{\sqrt{\vartheta}x}{b}} - m_1(\lambda+\sqrt{\vartheta}-2)} \\ &- \frac{6(-\lambda+\mu+1)^2\left(m_2(\lambda-\sqrt{\vartheta})e^{\frac{\sqrt{\vartheta}x}{b}} + m_1(\lambda+\sqrt{\vartheta})\right)^2}{\left[m_2(-\lambda+\sqrt{\vartheta}+2)e^{\frac{\sqrt{\vartheta}x}{b}} - m_1(\lambda+\sqrt{\vartheta}-2)\right]^2} - \lambda^2 + 6\lambda\mu - 2\mu(3\mu+1)\Bigg]. \end{aligned} \tag{3.22}$$

- If

$$(\lambda-2)(m_2-m_1) - \sqrt{\vartheta}(m_2+m_1) = 0,$$

then Eq (3.20) becomes

$$u_{1,1} = \frac{k^2\left(-3\vartheta\tanh^2\left(\frac{\eta\sqrt{\vartheta}}{2b}\right) + \lambda^2 - 4\mu\right)}{6b^2}. \tag{3.23}$$

- If

$$(\lambda-2)(m_2+m_1) - \sqrt{\vartheta}(m_2-m_1) = 0,$$

then Eq (3.20) becomes

$$u_{1,2} = \frac{k^2\left(-3\vartheta\coth^2\left(\frac{\eta\sqrt{\vartheta}}{2b}\right) + \lambda^2 - 4\mu\right)}{6b^2}. \tag{3.24}$$

Case 2. If

$$\vartheta = \lambda^2 - 4\mu < 0,$$

then

$$u_2 = \frac{k^2\left(-6b^2F^2(-\lambda+\mu+1)^2 + 6bFQ(\lambda-2\mu) - \lambda^2 + 6\lambda\mu - 2\mu(3\mu+1)\right)}{3b^2}, \tag{3.25}$$

where

$$F = \frac{S_1\cos(\frac{\sqrt{-\vartheta}}{2b}\eta) + S_2\sin(\frac{\sqrt{-\vartheta}}{2b}\eta)}{S_3\cos(\frac{\sqrt{-\vartheta}}{2b}\eta) + S_4\sin(\frac{\sqrt{-\vartheta}}{2b}\eta)}. \tag{3.26}$$

Substitute Eq (3.26) into Eq (3.25) to get

$$u_2 = \frac{k^2}{3b^2}\Bigg[\frac{6bQ(\lambda-2\mu)\left(S_1\cos\left(\frac{\eta\sqrt{-\vartheta}}{2b}\right)+S_2\sin\left(\frac{\eta\sqrt{-\vartheta}}{2b}\right)\right)}{S_3\cos\left(\frac{\eta\sqrt{-\vartheta}}{2b}\right)+S_4\sin\left(\frac{\eta\sqrt{-\vartheta}}{2b}\right)} - \lambda^2+6\lambda\mu-2\mu(3\mu+1)$$
$$-\frac{6b^2(-\lambda+\mu+1)^2\left(S_1\cos\left(\frac{\eta\sqrt{-\vartheta}}{2b}\right)+S_2\sin\left(\frac{\eta\sqrt{-\vartheta}}{2b}\right)\right)^2}{\left(S_3\cos\left(\frac{\eta\sqrt{-\vartheta}}{2b}\right)+S_4\sin\left(\frac{\eta\sqrt{-\vartheta}}{2b}\right)\right)^2}\Bigg], \tag{3.27}$$

- If

$$(\lambda-2)m_2+\sqrt{-\vartheta}\,m_1=0,$$

then Eq (3.25) becomes

$$u_{2,1} = \frac{k^2\left(-3\vartheta\tanh^2\left(\frac{\eta\sqrt{\vartheta}}{2b}\right)+\lambda^2-4\mu\right)}{6b^2}. \tag{3.28}$$

- If

$$(\lambda-2)m_1-\sqrt{-\vartheta}\,m_2=0,$$

then Eq (3.25) becomes

$$u_{2,2}(x,y,z,t) = \frac{k^2\left(-3\vartheta\coth^2\left(\frac{\eta\sqrt{\vartheta}}{2b}\right)+\lambda^2-4\mu\right)}{6b^2}. \tag{3.29}$$

- This detailed study helps us understand the physical processes better by looking at both the movement and mathematical features of these solutions. Using pictures, we make it easier to see how waves interact and what happens in complex situations. This visual approach makes it simpler to grasp the results and how they apply in real-world scenarios.

- To check that our solution is correct, an analytical technique is performed, namely the finite difference method with periodic boundary condition. The results from the simulation closely resemble the analytical solution, keeping the same shape and strength. This confirms that the soliton solution is accurate and reliable.

- Both methods work by finding a balanced solution and use certain types of solutions, which may exclude other possible solutions. It also involves turning the PDE into an ODE, which makes it less applicable for complicated or irregular equations. In those situations, other methods like analytical or numerical techniques might be better choices to get the exact solution.

4. Physical interpretation

The solutions to the (3+1)-dimensional KP equation form localized, stable wave patterns that exhibit solitons. These solutions can have multiple peaks that interact with each other, causing phases shifts and amplitudes. The additional spatial dimensions generate more complex wave patterns, such as

sideways oscillations and waves that combine localized and oscillatory behaviors. These characteristics highlight the complicated nonlinear systems in higher dimensions. In this section, we will discuss some of the solutions we found for the KP equation using graphs. We use mainly the GA method and the $\frac{G'}{bG'+G+a}$ expansion method to uncover soliton solutions. Depending on the parameters, these solutions describe waves that are focused in certain areas, wave packets that interact with each other, and waves that change in their side-to-side movement while moving mainly in one direction. These types of waves can represent stable patterns in shallow water waves in fluid dynamics, waves in plasma like ion-acoustic or Alfvén waves, and pulses of light in materials that respond to light in a non-linear way. In all these cases, the way the wave bends and spreads out is controlled by a balance between nonlinearity and dispersion. By selecting specific values of the parameters, we can obtain different types of solutions, such as bright, dark, and singular solitons. It is important to mention that the results and solutions we found in this paper are new and have never been shared before.

Figure 1 shows how the solution of the GA method behaves over time, with parameters set as follows:

$$k = 1,\ \ \rho = 0.05,\ \ y = 0, z = 0,\ \ \kappa = 0.25,\ \ \text{and}\ \ B = 3$$

for $-5 < x, t < 5$. We use three different time slots for two-dimensional representation. ρ is one of the parameters where the behavior of the graph changes. Figure 2 shows the solution of Eq 3.6 with parameter values

$$\kappa = 0.25,\ \ z = 0,\ \ B = 3,\ \ k = 1,\ \ y = 0,\ \ \text{and}\ \ \rho = 0.05.$$

The graph in $\rho = 0.5$ behaves as a bright soliton, whereas in $\rho = -0.1$, the singular soliton structure shows a sharp peak and sudden breaks. For Eq (3.8), the soliton solution is shown in Figure 3 with the parameter values

$$y = 0,\ \ z = 0,\ \ B = 3,\ \ \rho = 0.05,\ \ \kappa = 0.25,\ \ \text{and}\ \ k = 1.$$

Three different time intervals are used to check how soliton solutions behave over time for two-dimensional graphs. Parameter values

$$\rho = -0.01,\ \ \kappa = 0.25,\ \ k = 1,\ \ y = 0,\ \ z = 0,\ \ \text{and}\ \ B = 3$$

are used to show the solution of Eq (3.8) in Figure 4. Taking into account the above statement, we can say that for different values of ρ, different shapes of graphs are produced.

Figure 5 shows the behavior of the solution of Eq (3.12) of the $\frac{G'}{bG'+G+a}$ expansion method, with different parameter values

$$\lambda = 3,\ \ \mu = 1,\ \ m_1 = 2,\ \ \text{and}\ \ m_2 = -1$$

for $-10 < x, t < 10$. For Eq (3.17), the solution is shown in Figure 6 with parameter values

$$\lambda = 1,\ \ \mu = 1,\ \ m_1 = -2,\ \ \text{and}\ \ m_2 = 1.$$

Figure 7 shows the solution of Eq (3.22) with parameter values

$$m_1 = 2,\ \ m_2 = -1,\ \ \lambda = 3,\ \ \text{and}\ \ \mu = 1.$$

Figure 8 shows sharp peaks in a continuous way, which means it is stable and well behaved in a periodic manner for Eq (3.27). By changing the values of m_1, m_2, the graph demonstrates different behaviors.

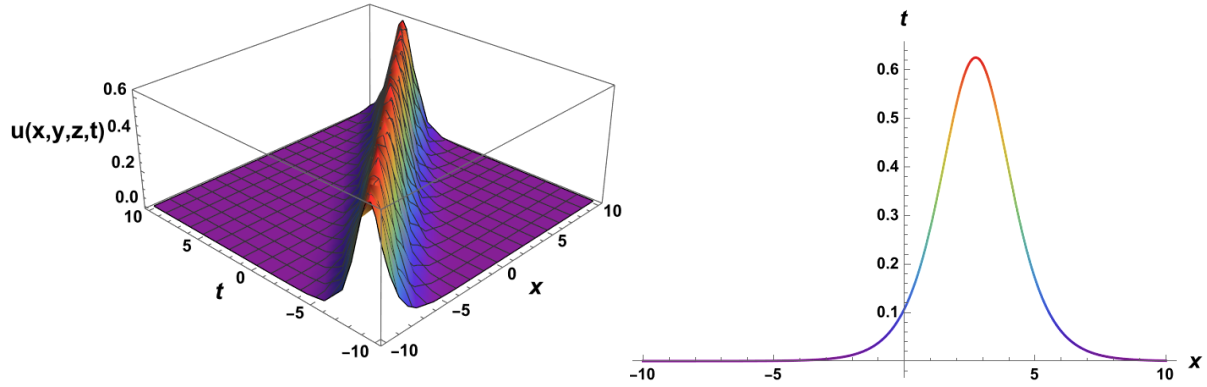

(a) **(b)**

Figure 5. $3D$ and $2D$ with $\lambda = 3$, $\mu = 1$, $m_1 = 2$, and $m_2 = -1$ for $-10 < x, t < 10$.

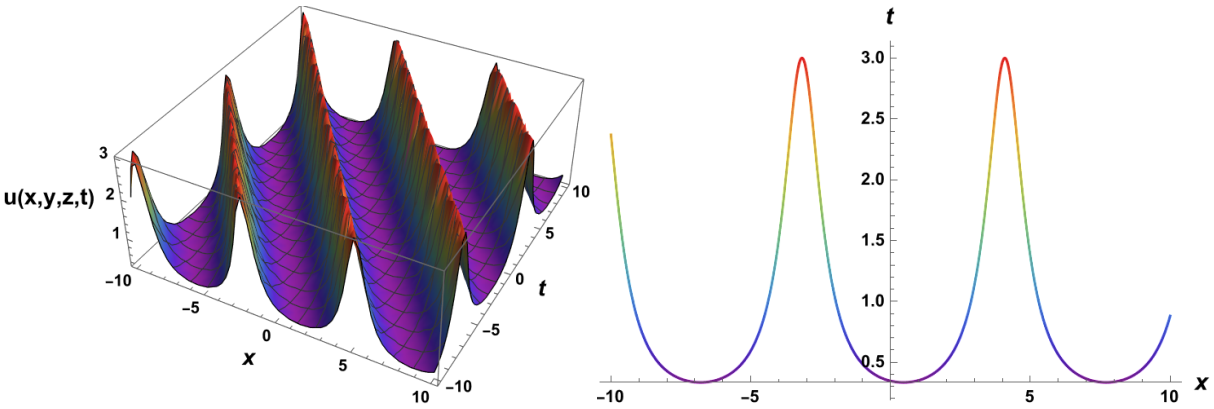

(a) **(b)**

Figure 6. $3D$ and $2D$with $\lambda = 1$, $\mu = 1$, $m_1 = -2$, and $m_2 = 1$ for $-10 < x, t < 10$.

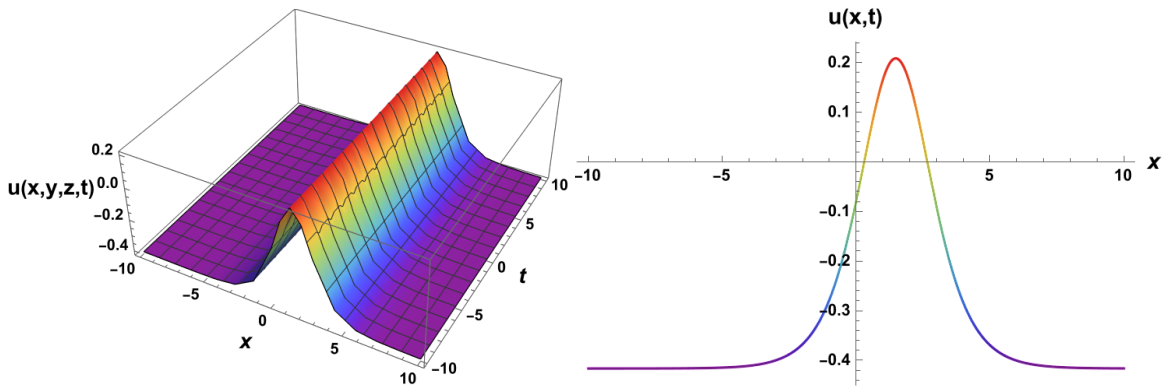

(a) **(b)**

Figure 7. $3D$ and $2D$ with $\lambda = 3$, $\mu = 1$, $m_1 = 2$, and $m_2 = -1$ for $-10 < x, t < 10$.

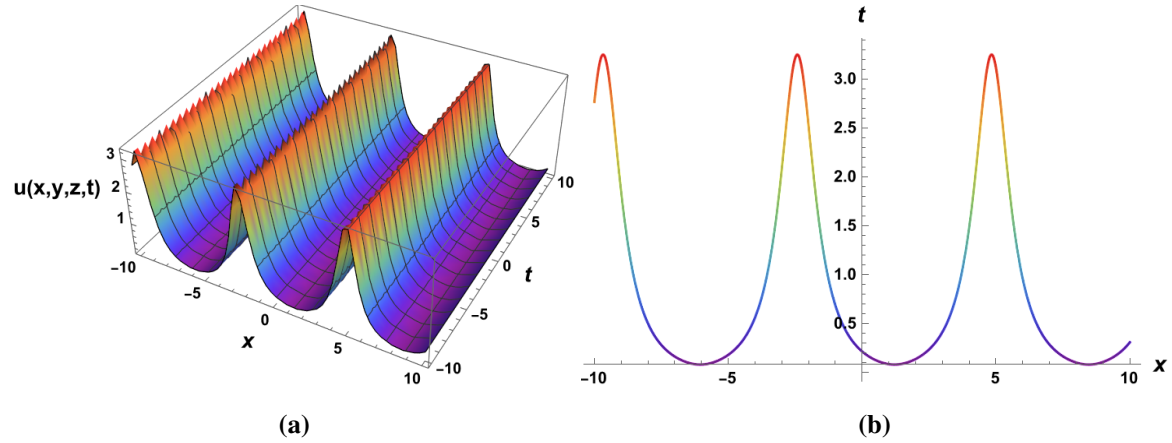

Figure 8. $3D$ and $2D$ with $\lambda = 1$, $\mu = 1$, $m_1 = -2$, and $m_2 = 1$ for $-10 < x, t < 10$.

For positive values of m_1 and negative m_2, the graph represents a bright soliton. When we change the signs of m_1 and m_2, it displays the periodic soliton structure. From this observation, we can say that different shapes of graphs are obtained for different values of m_1 and m_2.

5. Modulation instability

The balance between spreading out and bending effects causes modulation instability in steady states during many nonlinear processes. When a small disturbance is added, a continuous wave state grows rapidly, which is a fundamental nonlinear behavior. This leads to the continuous wave splitting into many very short pulses. In this section, we use the linear stability method to study the modulation instability of the KP equation. We look at the steady-state solution for Eq (1.2),

$$u = U(x, y, z, t) + n. \tag{5.1}$$

Then changing to linear form will give the next equations:

$$6nU_{xx}(x, y, z, t) - 3U_{zz}(x, y, z, t) - 3U_{yy}(x, y, z, t) + U_{xt}(x, y, z, t) + U_{xxxx}(x, y, z, t) = 0. \tag{5.2}$$

The wave transformation is

$$U(x, y, z, t) = P_1 e^{-i(fx+gy+dz-ht)} + Q_1 e^{i(fx+gy+dz-ht)}. \tag{5.3}$$

Substitute Eq (5.3) into (5.2), we get

$$\begin{aligned} &3d^2 P_1 e^{-i(dz+fx+gy-ht)} + 3d^2 Q_1 e^{i(dz+fx+gy-ht)} + f^4 P_1 e^{-i(dz+fx+gy-ht)} + f^4 Q_1 e^{i(dz+fx+gy-ht)} \\ &- 6f^2 n P_1 e^{-i(dz+fx+gy-ht)} - 6f^2 n Q_1 e^{i(dz+fx+gy-ht)} + 3g^2 P_1 e^{-i(dz+fx+gy-ht)} + 3g^2 Q_1 e^{i(dz+fx+gy-ht)} \\ &+ fh P_1 e^{-i(dz+fx+gy-ht)} + fh Q_1 e^{i(dz+fx+gy-ht)} = 0. \end{aligned} \tag{5.4}$$

Setting the determinant of the coefficient matrix equal to zero gives this relationship:

$$3d^2 + f^4 + 3g^2 + fh - 6f^2 n = 0. \tag{5.5}$$

After some simplification, we get

$$h \to \frac{-3d^2 - f^4 + 6f^2n - 3g^2}{f}. \tag{5.6}$$

It gives following dispersion relation:

$$\frac{-3d^2 - f^4 + 6f^2n - 3g^2}{f}. \tag{5.7}$$

The steady-state stability is shown by the dispersion relation (5.7). When the wave number is real, the steady state appears to be able to tackle small perturbation. However, when the wave number is imaginary, the steady state becomes unstable, and the disturbance grows exponentially. In this case, the growth rate is

$$\frac{-3d^2 - f^4 + 6f^2n - 3g^2}{f} < 0. \tag{5.8}$$

The dispersion relation illustrates how the growth rate $m(w)$ changes with the wave number w for different values of the parameter n. When $m(w)$ is positive, it indicates that the wave is unstable due to modulation instability, but when it is negative, the wave is stable. As the value of n increases in Figure 9, the range of unstable waves becomes wider, and the highest growth rate gets larger, indicating the stronger modulation effects. The sharp change near

$$w = 0$$

shows that long-wavelength disturbances play an important role in causing wave localization and forming patterns in KP wave behavior. A decrease in n in Figure 10 causes both the growth rate and the range of unstable wave numbers to decrease, which helps reduce modulation instability. As a result, the wave propagation becomes more stable and less likely to form localized patterns or structures.

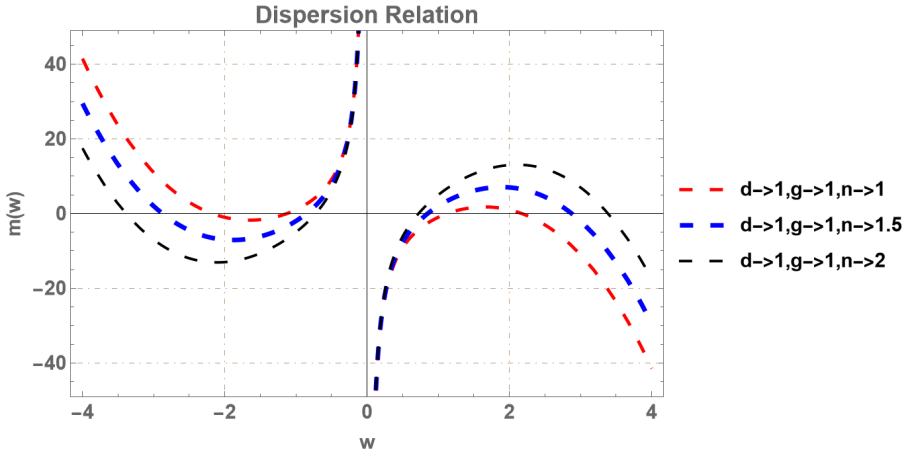

Figure 9. Dispersion relation vs wave number for increasing n.

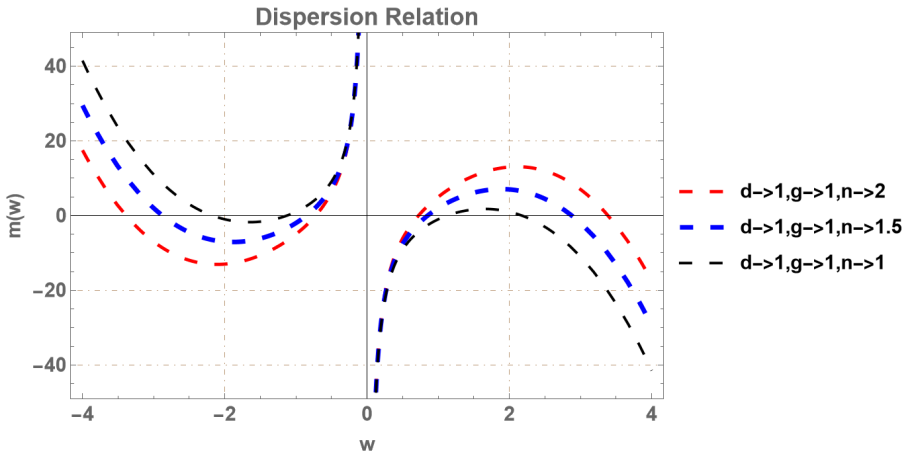

Figure 10. Dispersion curve showing the dependency of wave stability for decreasing n.

6. Conclusions

In this piece of research, we studied the (3+1)-dimensional KP equation by using the GA method and the $\frac{G'}{bG'+G+a}$ expansion method. With the implementation of these methods, the solutions emerged in the form of hyperbolic, trigonometric, and rational functions. The results of our study have many applications in plasma physics, and our suggested mathematical techniques are stronger as a result. This suggests that these techniques are more reliable and successful in identifying precise solutions to nonlinear PDEs. These techniques can be used for create a variety of original solutions. With different parameter values in figures, these solutions showed solitary, bright, singular, and periodic solitons, which have many applications in physics. These techniques can be used to other similar nonlinear equations and systems of equations. These methods can be naturally extended to other multidimensional nonlinear models, such as the (3+1)-dimensional Wazwaz–Benjamin–Bona–Mahony equations or the (3+1)-dimensional Zakharov–Kuznetsov equations in plasma physics. They are ideal for studying complicated wave phenomena in such higher–dimensional systems because of their methodical derivation procedure and capacity to produce a variety of correct solutions. The solutions discovered in this study were found using the Mathematica package program. In this work, we were able to get precise traveling wave solutions for this equation. Many of the results are original solutions that have never been put forth in the literature.

Use of Generative-AI tools declaration

The author declares he has not used artificial intelligence (AI) tools in the creation of this article.

Acknowledgments

The author is thankful to the Deanship of Graduate Studies and Scientific Research at University of Bisha for supporting this work through the Fast-Track Research Support Program.

Conflict of interest

The author declares that there is no conflict of interest.

References

1. M. A. Abdou, An analytical method for space-time fractional nonlinear differential equations arising in plasma physics, *J. Ocean Eng. Sci.*, **2** (2017), 288292. https://doi.org/10.1016/j.joes.2017.09.002
2. L. Akinyemi, H. Rezazadeh, S. W. Yao, M. A. Akbar, M. M. Khater, A. Jhangeer, et al., Nonlinear dispersion in parabolic law medium and its optical solitons, *Results Phys.*, **26** (2021), 104411. https://doi.org/10.1016/j.rinp.2021.104411
3. C. Qiao, X. Long, L. Yang, Y. Zhu, W. Cai, Calculation of a dynamical substitute for the real earth-moon system based on Hamiltonian analysis, *Astrophys. J.*, **991** (2025), 46. https://doi.org/10.3847/1538-4357/adf73a
4. M. Tanaka, The stability of solitary waves, *Phys. Fluids*, **29** (1986), 650–655. https://doi.org/10.1063/1.865459
5. J. E. Allen, The early history of solitons (solitary waves), *Phys. Scr.*, **57** (1998), 436. https://doi.org/10.1088/0031-8949/57/3/016
6. K. K. Ali, M. S. Mohamed, M. Maneea, Optimal homotopy analysis method for (2+1) time-fractional nonlinear biological population model using-transform, *AIMS Math.*, **9** (2024), 32757–32781. https://doi.org/10.3934/math.20241567
7. N. Raza, A. Javid, Dynamics of optical solitons with Radhakrishnan–Kundu–Lakshmanan model via two reliable integration schemes, *Optik*, **178** (2019), 557–566. https://doi.org/10.1016/j.ijleo.2018.09.133
8. A. M. Wazwaz, The tanh–coth method for solitons and kink solutions for nonlinear parabolic equations, *Appl. Math. Comput.*, **188** (2007), 1467–1475. https://doi.org/10.1016/j.amc.2006.11.013
9. M. J. Ablowitz, H. Segur, *Solitons and the inverse scattering transform*, Philadelphia, 1981. https://doi.org/10.1137/1.9781611970883
10. M. A. Noor, S. T. Mohyud-Din, A. Waheed, E. A. Al-Said, Exp-function method for traveling wave solutions of nonlinear evolution equations, *Appl. Math. Comput.*, **216** (2010), 477–483. https://doi.org/10.1016/j.amc.2010.01.042
11. R. Conte, M. Musette, Link between solitary waves and projective Riccati equations, *J. Phys. A*, **25** (1992), 5609. https://doi.org/10.1088/0305-4470/25/21/019
12. A. T. Ali, New generalized Jacobi elliptic function rational expansion method, *J. Comput. Appl. Math.*, **235** (2011), 4117–4127. https://doi.org/10.1016/j.cam.2011.03.002
13. S. F. Tian, M. J. Xu, T. T. Zhang, A symmetry-preserving di erence scheme and analytical solutions of a generalized higher-order beam equation, *Proc. R. Soc. A*, **477** (2021), 20210455. https://doi.org/10.1098/rspa.2021.0455

14. E. M. Zayed, K. A. Gepreel, R. M. Shohib, M. E. Alngar, Y. Yildirim, Optical solitons for the perturbed Biswas-Milovic equation with Kudryashovs law of refractive index by the unified auxiliary equation method, *Optik*, **230** (2021), 166286. https://doi.org/10.1016/j.ijleo.2021.166286

15. T. A. Sulaiman, A. Yusuf, Dynamics of lump-periodic and breather waves solutions with variable coecients in liquid with gas bubbles, *Waves Random Complex Media*, **33** (2014), 1085–1098. https://doi.org/10.1080/17455030.2021.1897708

16. A. Zafar, M. Shakeel, A. Ali, L. Akinyemi, H. Rezazadeh, Optical solitons of nonlinear complex Ginzburg–Landau equation via two modified expansion schemes, *Opt. Quant. Electron.*, **54** (2022), 5. https://doi.org/10.1007/s11082-021-03393-x

17. I. S. O'Keir, E. J. Parkes, The derivation of a modified Kadomtsev–Petviashvili equation and the stability of its solutions, *Phys. Scr.*, **55** (1997), 135. https://doi.org/10.1088/0031-8949/55/2/003

18. S. F. Tian, P. L. Ma, On the quasi-periodic wave solutions and asymptotic analysis to a (3+1)-dimensional generalized Kadomtsev–Petviashvili equation, *Commun. Theor. Phys.*, **62** (2014), 245. https://doi.org/10.1088/0253-6102/62/2/12

19. M. J. Ablowitz, H. Segur, On the evolution of packets of water waves, *J. Fluid Mech.*, **92** (1979), 691–715. https://doi.org/10.1017/S0022112079000835

20. G. P. Agrawal, Nonlinear fiber optics, In: P. L. Christiansen, M. P. Sørensen, A. C. Scott, *Nonlinear science at the dawn of the 21st century*, Springer Berlin, 2000. https://doi.org/10.1007/3-540-46629-0_9

21. R. Grimshaw, Internal solitary waves, In: R. Grimshaw, *Environmental stratified flows*, Springer, 2001. https://doi.org/10.1007/0-306-48024-7_1

22. B. Dorizzi, B. Grammaticos, A. Ramani, P. Winternitz, Are all the equations of the Kadomtsev–Petviashvili hierarchy integrable? *J. Math. Phys.*, **27** (1986), 2848–2852. https://doi.org/10.1063/1.527260

23. T. Alagesan, A. Uthayakumar, K. Porsezian, Painlevé analysis and Bäcklund transformation for a three-dimensional Kadomtsev–Petviashvili equation, *Chaos Solitons Fract.* **8** (1997), 893–895. https://doi.org/10.1016/S0960-0779(96)00166-X

24. W. X. Ma, Comment on the (3+1)-dimensional Kadomtsev–Petviashvili equations *Commun. Nonlinear Sci. Numer. Simul.*, **16** (2011), 2663–2666. https://doi.org/10.1016/j.cnsns.2010.10.003

25. G. Q. Xu, A. M. Wazwaz, A new (n+1)-dimensional generalized Kadomtsev–Petviashvili equation: integrability characteristics and localized solutions, *Nonlinear Dyn.*, **111** (2023), 9495–9507. https://doi.org/10.1007/s11071-023-08343-8

26. Y. Li, F. Li, M. Tian, Y. Yao, (3+1)-dimensional-modified Kadomtsev–Petviashvili equation and its ∂-formalism, *Proc. Soc.*, **481** (2025), 20250342. https://doi.org/10.1098/rspa.2025.0342

27. W. Alhejaili, A. Wazwaz, S. El-Tantawy, New extended (3+1)-dimensional KP-type equations: Painlevé integrability, multi-solitons, and lump solutions, *Rom. Reports Phys.*, **77** (2025), 109. https://doi.org/10.59277/romrepphys.2025.77.109

28. J. M. A. Ahamed, R. Sinuvasan, Exploring the (3+1)-generalized Kadomtsev–Petviashvili equation: symmetries, reductions, and exact solutions, *Phys. Scr.*, **100** (2025), 055210. https://doi.org/10.1088/1402-4896/adc638

29. W. Mohammed, A. Khalifa, H. Alshammari, H. Ahmed, M. Algolam, R. Elbarougy, et al., Innovative solitary wave solutions for the (3+1)-dimensional Boussinesq Kadomtsev–Petviashvili–type equation derived via the improved modified extended tanh-function method, *Eur. J. Pure Appl. Math.*, **18** (2025), 3. https://doi.org/10.29020/nybg.ejpam.v18i3.6490

30. W. Alhejaili, A. M. Wazwaz, S. A. El-Tantawy, On the multiple soliton and lump solutions to the (3+1)-dimensional Painlevé integrable Boussinesq-type and KP-type equations, *Rom. Reports Phys.*, **76** (2024), 115. https://doi.org/10.59277/romrepphys.2024.76.115

31. C. Bhan, R. Karwasra, S. Malik, S. Kumar, A. H. Arnous, N. A. Shah, et al., Bifurcation, chaotic behavior and soliton solutions to the KP-BBM equation through new Kudryashov and generalized Arnous methods, *AIMS Math.*, **9** (2024), 8749–8767. https://doi.org/10.3934/math.2024424

32. N. Raza, S. S. Kazmi, G. A. Basendwah, Dynamical analysis of solitonic, quasi-periodic, bifurcation and chaotic patterns of Landau–Ginzburg–Higgs model, *J. Appl. Anal. Comput.*, **14** (2024), 197–213. https://doi.org/10.11948/20230137

Appendix

Computational details

Mathematica commands for Figures 1–4

```
(* Traveling wave solution *)
u[x_,y_,z_, t_] := \frac{32 \kappa ^2 k^2 \rho
\ln^2(B) B ^{2 \eta}}{\left(\rho +4 \kappa ^2 \ln^2(B)
B ^{2 \eta}\right)^2}

(* Parameters used in Figure 1 *)
\rho = 0.5; k = 1; \kappa = 0.25; y= 0; z = 0;B = 3

Plot3D[u[x_,y_,z_, t_], {x, -5,
  5}, {t, -10, 10}, ColorFunction -> (ColorData["Rainbow"]),
 AxesLabel -> {Style[x, FontSize -> 14], Style[t, FontSize -> 14],
   Style["u(x,y,z,t)", FontSize -> 14]},
 LabelStyle -> Directive[Black, Bold], PlotStyle -> "Surface",
 PlotRange -> All]
```

All the figures are generated by using this command with different parameter values, which is illustrated in section.